



A new theory for electroded piezoelectric plates and its finite element application for the forced vibrations of quartz crystal resonators

Ji Wang^{a,*}, Jiun-der Yu^a, Yook-Kong Yong^b, Tsutomu Imai^c

^a*Epson Palo Alto Laboratory, 3145 Porter Drive, Suite 104, Palo Alto, CA 94304-1224, USA*

^b*Department of Civil and Environmental Engineering, Rutgers University, Piscataway, NJ 08855-0909, USA*

^c*EM Technology Laboratory, Seiko Epson Corporation, 3-3-5 Owa, Suwa-shi, Nagano-ken 392, Japan*

Received 12 November 1998; in revised form 26 August 1999

Abstract

For crystal resonators, it is always desirable to calculate the electric properties accurately for application purposes. Such calculations have been done with analytical solutions from approximate equations and simplified models with good results, but for better consideration of the actual resonators, finite element method has been used for the free vibration analysis with excellent results to aid the analysis and design. The finite element analysis based on the higher order Mindlin plate theory is particularly effective and easy to implement and expand. As an extension of the Mindlin plate theory based finite element analysis of crystal resonators, a new theory for the electroded plates is derived and the piezoelectrically forced vibrations are formulated and implemented in this paper in a manner similar to our previous work. The effect of the electrodes and the electric boundary conditions are taken into consideration through the modification of the higher order plate equations by changing the expansion function of the electric potential for this particular problem. Through the conventional discretization of the new plate theory, the linear equations for the piezoelectric plate under thickness excitation are constructed and solved with efficient numerical computation techniques such as the sparse matrix handling. The solutions of mechanical displacement and electric potential are then used for the computation of the capacitance ratio of the electroded plate with emphasis on its derivation with the two-dimensional plate theory. The applications of these results in crystal resonator modeling are discussed and demonstrated in detail. Numerical examples showing good predictions of the resonance frequency and capacitance ratio of electroded crystal plates of *AT*-cut quartz are presented with experimental data. Published by Elsevier Science Ltd.

Keywords: Plate; Mindlin; Crystal; Piezoelectric; Resonator; Vibration; Capacitance; Finite; Element; Electrode

* Corresponding author. Tel.: +1-650-843-8336; fax: +1-650-843-9106.

E-mail addresses: jiwang@erd.epson.com (J. Wang), jdyu@erd.epson.com (J. Yu), yong@jove.rutgers.edu (Y.-K. Yong), imai.t-sutomu@exc.epson.co.jp (T. Imai).

1. Introduction

Two-dimensional plate theories have been specifically developed for and widely used in the study of vibrations of piezoelectric plates and crystal resonators. The extensive theoretical development has been covering many aspects on the analytical solutions including the resonance frequency, mechanical effects of electrodes, thermal effects, and piezoelectrically excited vibrations, to name a few. The solutions from these two-dimensional approximate theories, through proper combination and interpretation, can be used to calculate the basic properties, or the parameters, of crystal resonators. Furthermore, many physical phenomena associated with vibrations of crystal resonators, such as the coupling of modes and the frequency discontinuity (activity dip) due to thermal effect, can also be explored with these solutions and considerations of other complication factors. This demonstrates the effectiveness and importance of the plate theory based vibration analysis in the practical modeling of crystal resonators.

Because of the complexity of plate vibrations, which includes the multiple variables, complicated boundary conditions, and complications of a plate with the presence of electrodes and mountings, analytical solutions cannot be obtained for the two-dimensional problems even for equations in the lowest order. For simplicity, but also adequately accurate for applications such as characterization, the equations have been truncated to retain only the essential variables and correction factors which have been introduced for the straight-crested wave solutions that neglect the effect of one spatial coordinate for some special cases. Indeed, these solutions have been proven to be accurate and efficient in certain applications, particularly if the resonance frequency, frequency–temperature relations, and capacitances are concerned for plates with simple geometry. With a small number of equations of dominant modes and affordable computational costs, these solutions can be used to capture the essential characteristics of the resonators to aid the development efforts in conjunction with necessary experimental work. A precise and rigorous solution requires the adoption of the finite element method, which can be especially challenging due to the extremely high vibration frequency. The advantage of such an analysis, on the other hand, is quite obvious, if the accurate solutions of the vibrations are taken into account. However, it should be pointed out that even the finite element analysis, in most cases, are based on the approximate two-dimensional equations, which inevitably have been compensated with correction factors for the truncations. In addition, some complications such as the consideration of electrodes as mass loading, is also treated with approximation. These facts remind us that certain approximations in the implementation of the two-dimensional theory are feasible and accurate, thus making the results practical and useful in most applications.

For the piezoelectrically excited vibrations of a crystal resonator, further consideration on the electric boundary condition which requires that the electric potential on the electrodes must be equal has to be satisfied. This can be difficult to accommodate because in plate theories like Mindlin (1955, 1972) or Lee et al. (1987), the potential has been expanded into either power series or trigonometric series involving higher order terms. Given the fact that the electric effect will affect the equations of charge through the electric displacement on the surface, a relation between the electric potential components and the electric displacement on the faces of the plate has to be established. One of the solutions is to expand the electric displacement rather than the potential, as demonstrated by Tiersten and Mindlin (1962) and Tiersten (1969), so the electric potential on the faces can be incorporated into the electric displacement. Also, the effect of the potential on the face tractions due to piezoelectricity may need to be considered. For the lower order theory such as the first-order, the relation can be relatively simple because the constant or linear expansion (in thickness coordinate) of potential will be able to provide necessary equations for the solution as demonstrated by Tiersten (1969), Mindlin (1972) and Lee et al. (1987). If the higher order theory involving the potential terms is required, we have found that such a relation is hard to construct without creating further doubts on the applicability of the theory itself. This problem has been noticed and investigated by Tiersten (1993) and Lee and Yu (1998) by using special expansion

schemes which can satisfy the constant potential condition on the electrodes without requiring any approximate relationship between the potential and the electric displacement. In fact, all these similar expansion schemes have specified, not surprisingly, that the higher order electric potentials (from the second and up) will disappear on the electrodes. This is certainly the best approach to handle the driving voltage on the electrodes, because there is no approximation procedure involved in order to preserve the constant potential on the faces.

However, we found that these expansions have disregarded the original scheme employed by Mindlin (1972), in which the electric potential is in power series of the thickness coordinate, thus effectively making the new theory completely irrelevant to the Mindlin plate theory for plates without electrodes. In practical applications, the plates are usually partially electroded for energy trapping and other purposes. The analysis of such partially electroded plates require that the equations in the two regions, unelectroded and electroded, should be compatible so the proper continuity conditions can be enforced in both one- and two-dimensional problems. For this consideration, we start the new theory by closely following Mindlin. In fact, the adoption of the new expansion does not change the definitions of the higher order potentials at all. The expansion of the potential is modified based on the known requirement on the electrodes, but the original definition of the higher order components of both mechanical and electric potential are preserved through this process. As a standard procedure, the two-dimensional equations are deduced from the three-dimensional variational equations of motion and charge. The two-dimensional stress, electric field, and electric displacement tensors are modified and redefined based on the expansion scheme. Finally, a complete two-dimensional theory for electroded piezoelectric plates, suitable for the high frequency vibrations of crystal resonators under thickness excitation, are established. Furthermore, as we emphasized earlier, this equation is compatible with the Mindlin plate theory so it would be more suitable for partially electroded plates.

It should be pointed out that we do not precede to the truncation, simplification, and the one-dimensional solutions of the equations after its completion. Instead, we implemented the theory in the finite element analysis procedure as part of our effort in the modeling of crystal resonators, as demonstrated in our previous paper (Wang et al., 1999), to establish the framework of the implementation of the higher order plate theory and the generalized formulation for the piezoelectric plates. We presented our results based on the finite element computation for comparison with known experimental data. As we concluded in our earlier study, the consideration of the electrodes electrically do not change the frequency characteristics much, again showing that the piezoelectric effects in such analysis are negligible. This also reminds us that we may be able to use the solutions from the mechanical vibrations for the accurate predictions of the electric properties as well. We also derived the equation for the capacitance ratio from the new equations and implemented it in the finite element analysis. The adoption of the third-order plate theory is based on an earlier study (Yong et al., 1996b) on the accuracy of different plate theories (Mindlin and Lee) in the prediction of the resonance frequency, as we have discussed earlier (Yong et al., 1996a; Wang et al., 1999). The results presented in this paper, as we expected, are in close agreement with the experimental data.

2. 2D equations with the consideration of electrodes

It has been widely known that in the derivation of the two-dimensional higher order Mindlin plate theory for piezoelectric plates, the mechanical displacements and electric potential are expanded into power series of the thickness coordinate as

$$u_j = \sum_{n=0}^{\infty} x_2^n u_j^{(n)}, \quad \phi = \sum_{n=0}^{\infty} x_2^n \phi^{(n)}, \tag{1}$$

where $u_j^{(n)}$ and $\phi^{(n)}$ are the n th-order displacement and electric potential, respectively. The coordinate system of the plate, which is considered fully electroded here, is shown in Fig. 1. The Mindlin plate theory, particularly with its extension to higher order variables, has wide applications in the high frequency vibrations of piezoelectric plates for crystal resonator analysis. Truncated equations with selected vibration modes, typically thickness-shear and flexure, from Mindlin plate theory based on (1) have been applied to forced vibrations of crystal plate resonators by Mindlin (1984) and Sekimoto et al. (1992) and from Lee plate theory (Lee et al., 1987) by Lee and Wang (1996), Wang and Momosaki (1997), finally by Lee and Lin (1998). However, it should be noted that an approximation has been made in the consideration of the driving voltage on the electrodes. While the approximating procedure, as shown by Lee et al. (1987), is relatively simple for the first-order equations, an extension to include higher order terms is difficult to obtain.

2.1. The electric potential expansion

For piezoelectric plates with electroded faces, it is essential to consider the additional requirement that the electric potential on the faces should be constant. With the potential expansion given in (1)₂, such a condition can only be satisfied with

$$\phi(b) = \sum_{n=0}^{\infty} b^n \phi^{(n)},$$

$$\phi(-b) = \sum_{n=0}^{\infty} (-b)^n \phi^{(n)}, \quad (2)$$

where $\phi(b)$ and $\phi(-b)$ are the driving voltages on the upper and lower faces ($x_2 = \pm b$). Because the even and odd terms in (2) can be cancelled through summation and subtraction, a relation showing that the higher order potentials are not totally independent among the potential terms can be established. The dependence of the potentials will provide further opportunity for the modification of the potential expansion and thus the equations. To start, we obtain $\phi^{(0)}$ and $\phi^{(1)}$ from (2) as

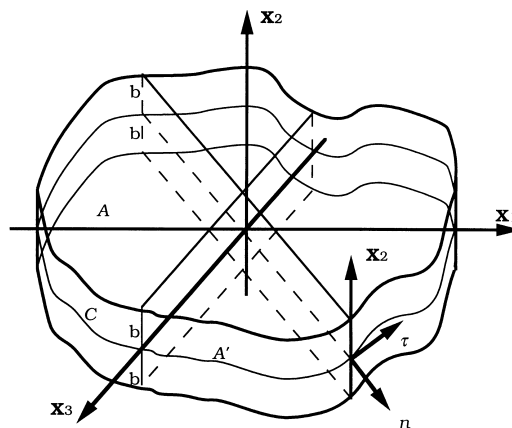


Fig. 1. A quartz crystal plate.

$$\phi^{(0)} = \phi_0 - \sum_{n=0}^{\infty} b^{2(n+1)} \phi^{(2n+2)},$$

$$\phi^{(1)} = \frac{\phi_1}{b} - \sum_{n=0}^{\infty} b^{2(n+1)} \phi^{(2n+3)},$$

$$\phi_0 = \frac{1}{2}[\phi(b) + \phi(-b)], \quad \phi_1 = \frac{1}{2}[\phi(b) - \phi(-b)]. \tag{3}$$

This shows that at least the zeroth- and first-order potentials, $\phi^{(0)}$ and $\phi^{(1)}$, can be expressed in terms of higher order potentials and the voltage on faces.

Through the substitution of (3) back to (1)₂, we have the new electric potential expansion upon satisfying the equal potential conditions on the faces as

$$\phi = \phi_0 + \frac{x_2}{b} \phi_1 + \sum_{n=0}^{\infty} (x_2^{2(n+1)} - b^{2(n+1)}) (\phi^{(2n+2)} + x_2 \phi^{(2n+3)}), \tag{4}$$

for electroded plates. For a closer look, the first few terms up to the third-order power series are

$$\phi = \phi_0 + \frac{x_2}{b} \phi_1 + (x_2^2 - b^2) \phi^{(2)} + x_2 (x_2^2 - b^2) \phi^{(3)}. \tag{5}$$

It is clearly shown that the face conditions are fully accommodated through the precise representation of the voltage on the electrodes. The replacement of the power series by a polynomial which vanishes on both faces ensures that only the constant terms, which are determined by the driving voltage, will determine the potential distribution. The effect of the higher order terms are limited to the potential distribution in the interior of the crystal plate. As a result, it is easy to understand that the relationship between the electric displacement and the potential is no longer needed. This, as we stated before, is the result we are actually looking for.

Although the expansion scheme we devise and present here is through a systematic derivation, concepts like this have been pioneered by other authors earlier. In the consideration of the vibrations of piezoelectric plates in large electric fields, Tiersten (1993) has essentially employed the same expansion and derived the equations up to the third-order displacement and potential. In the study of a piezoelectric plate with graded material properties across the thickness, Lee and Yu (1998) used the same expansion with slightly different notations. In essence, the same polynomial, $x_2^2 - b^2$, is present in all the expansions to take care of the face conditions of the electric potential, while the potential terms are different with a constant scaling factor. Tiersten’s equations are expanded to include cubic electrical nonlinearity by Yang (1999). In this paper, the same notations and procedure employed by Mindlin (1955) are inherited so the resulting equations can be used, as we also intended, for plates with partial electrodes and finite element implementation. However, for expansion of the potential higher than the third-order, the polynomials we employed here will be completely different from others, and a straightforward scaling of the potential terms will be impossible.

2.2. Two-dimensional equations

Through the examination of the expansion in (5), we can observe that only the constant terms are kept in the first-order equations. For the third-order expansion, we have

$$\delta\phi = (x_2^2 - b^2)\delta\phi^{(2)} + x_2(x_2^2 - b^2)\delta\phi^{(3)},$$

$$E_k = (x_2^2 - b^2)E_k^{(2)} + x_2(x_2^2 - b^2)E_k^{(3)},$$

$$E_2 = -\frac{\phi_1}{b} + 2x_2E_2^{(2)} + (3x_2^2 - b^2)E_2^{(3)}. \quad (6)$$

Apparently, we have defined the higher order electric fields related to the potential components in the above equation as

$$E_k^{(n)} = -\phi_{,k}^{(n)}, \quad E_2^{(n)} = -\phi^{(n)}, \quad n = 2, 3; k = 1, 3. \quad (7)$$

Since the mechanical displacements will remain unchanged, it should be kept in mind that the mechanical equations of motion should remain the same. However, the electric potentials in the stress terms should take new forms due to the changes in the electric field. For the derivation of the new two-dimensional constitutive equations, we write out the following three-dimensional ones for later use

$$T_p = c_{pq} \sum_{m=0}^{\infty} x_2^m S_q^{(m)} + e_{kp} \left[(x_2^2 - b^2)\phi_{,k}^{(2)} + x_2(x_2^2 - b^2)\phi_{,k}^{(3)} \right] + e_{2p} \left[\frac{\phi_1}{b} + 2x_2\phi^{(2)} + (3x_2^2 - b^2)\phi^{(3)} \right],$$

$$D_i = e_{iq} \sum_{m=0}^{\infty} x_2^m S_q^{(m)} - \epsilon_{ik} \left[(x_2^2 - b^2)\phi_{,k}^{(2)} + x_2(x_2^2 - b^2)\phi_{,k}^{(3)} \right] - \epsilon_{i2} \left[\frac{\phi_1}{b} + 2x_2\phi^{(2)} + (3x_2^2 - b^2)\phi^{(3)} \right],$$

$$p, q = 1, 2, 3, 4, 5, 6; i = 1, 2, 3; k = 1, 3, \quad (8)$$

where T_p , D_i , $S_p^{(n)}$, c_{pq} , e_{kp} , and ϵ_{ij} are stress, electric displacement vector, n th-order strain, elastic constant tensor, piezoelectric constant tensor, and dielectric constant tensor, respectively, without further elaboration. The n th-order strain tensor based on the power series expansion of mechanical displacements in (1)₁ is defined (Wang et al., 1999) as

$$S_{ij}^{(n)} = \frac{1}{2} \left[u_{i,j}^{(n)} + u_{j,i}^{(n)} + (n+1) \left(\delta_{i2} u_j^{(n+1)} + \delta_{j2} u_i^{(n+1)} \right) \right]. \quad (9)$$

By taking the standard procedure for the derivation of the two-dimensional plate theory from the three-dimensional equations of motion (Mindlin, 1972, 1984), in the third-order case, we have the two-dimensional constitutive equations

$$T_p^{(n)} = \int_{-b}^b T_p x_2^2 dx_2 = \int_{-b}^b \left\{ c_{pq} \sum_{m=0}^{\infty} x_2^m S_q^{(m)} + e_{kp} \left[(x_2^2 - b^2)\phi_{,k}^{(2)} + x_2(x_2^2 - b^2)\phi_{,k}^{(3)} \right] + e_{2p} \left[\frac{\phi_1}{b} + 2x_2\phi^{(2)} + (3x_2^2 - b^2)\phi^{(3)} \right] \right\} x_2^n dx_2$$

$$= c_{pq} \sum_{m=0}^{\infty} B_{mn} S_q^{(m)} - 2B_{1n} e_{2p} E_2^{(2)} - (B_{2n} - B_{0n} b^2) e_{kp} E_k^{(2)} - (B_{3n} - B_{1n} b^2) e_{kp} E_k^{(3)}$$

$$- (3B_{2n} - B_{0n} b^2) e_{2p} E_2^{(3)} + e_{2p} \frac{\phi_1}{b} B_{0n}, \quad (10)$$

where the integral constant is

$$B_{mn} = \begin{cases} \frac{2b^{m+n+1}}{m+n+1}, & m+n = \text{even}, \\ 0, & m+n = \text{odd}. \end{cases} \tag{11}$$

For the third-order theory, the two-dimensional constitutive relations are

$$\begin{aligned} T_p^{(0)} &= c_{pq} \left(2bS_q^{(0)} + \frac{2b^3}{3}S_q^{(2)} \right) + \frac{4b^3}{3}e_{kp}E_k^{(2)} + 2e_{2p}\phi_1, \\ T_p^{(1)} &= c_{pq} \left(\frac{2b^3}{3}S_q^{(1)} + \frac{2b^5}{5}S_q^{(3)} \right) - \frac{4b^3}{3}e_{2p}E_2^{(2)} + \frac{4b^5}{15}e_{kp}E_k^{(3)}, \\ T_p^{(2)} &= c_{pq} \left(\frac{2b^3}{3}S_q^{(0)} + \frac{2b^5}{5}S_q^{(2)} \right) + \frac{4b^5}{15}e_{kp}E_k^{(2)} - \frac{8b^5}{15}e_{2p}E_2^{(3)} + \frac{2b^2}{3}e_{2p}\phi_1, \\ T_p^{(3)} &= c_{pq} \left(\frac{2b^5}{5}S_q^{(1)} + \frac{2b^7}{7}S_q^{(3)} \right) - \frac{4b^5}{5}e_{2p}E_2^{(2)} + \frac{4b^7}{35}e_{kp}E_k^{(3)}. \end{aligned} \tag{12}$$

It should be noted that the prescribed driving voltage ϕ_1 appears in these equations.

Through proper arrangement and combination, the previous equations can be expressed in tensor notations as

$$\mathbf{T}^{(n)} = B_{mn}\mathbf{cS}^{(m)} - \mathbf{e}_n^{(2)}\mathbf{E}^{(2)} - \mathbf{e}_n^{(3)}\mathbf{E}^{(3)} - \mathbf{e}^{(n)}\phi_1, \quad n = 0, 1, 2, 3. \tag{13}$$

The definitions of the two-dimensional stress, strain, electric field vector, and the material constant matrices, will be given and explained in a later section.

For the two-dimensional charge equations, we need to start from the variational equation of charge to consider the changes in the potential expansion. The three-dimensional charge equation for a finite volume is

$$\int_V D_{i,i} \delta\phi \, dV = 0. \tag{14}$$

By using the potential variation in (6)₁, this equation can be written as

$$\int_A \int_{-b}^b D_{i,i} \left[(x_2^2 - b^2)\delta\phi^{(2)} + x_2(x_2^2 - b^2)\delta\phi^{(3)} \right] dx_2 \, dA = 0. \tag{15}$$

For the arbitrary variation of $\delta\phi^{(2)}$ and $\delta\phi^{(3)}$, we must have

$$\begin{aligned} \int_A \int_{-b}^b D_{i,i} (x_2^2 - b^2)\delta\phi^{(2)} \, dx_2 \, dA &= 0, \\ \int_A \int_{-b}^b D_{i,i} x_2(x_2^2 - b^2)\delta\phi^{(3)} \, dx_2 \, dA &= 0, \end{aligned} \tag{16}$$

or

$$\int_A \left(D_{i,i}^{(2)} - \bar{D}_2^{(2)} \right) \delta \phi^{(2)} dA = 0,$$

$$\int_A \left(D_{i,i}^{(3)} - \bar{D}_2^{(3)} \right) \delta \phi^{(3)} dA = 0, \quad (17)$$

where the two-dimensional electric displacement components in (17) are defined, with the use of (8)₂, as

$$D_i^{(2)} = \int_{-b}^b D_i(x_2^2 - b^2) dx_2 = -e_{ip} \sum_{m=0, 2, 4, \dots}^{\infty} \frac{4b^{m+3}}{(m+3)(m+1)} S_p^{(m)} - \frac{16b^5}{15} \epsilon_{ki} \phi_{,k}^{(2)} - \frac{8b^5}{15} \epsilon_{2i} \phi^{(3)} + \frac{4b^2}{3} \epsilon_{2i} \phi_1,$$

$$\bar{D}_2^{(2)} = \int_{-b}^b 2x_2 D_2 dx_2 = 2e_{2p} \sum_{m=0}^{\infty} B_{1m} S_p^{(m)} - \frac{8b^3}{3} \epsilon_{22} \phi^{(2)} + \frac{8b^5}{15} \epsilon_{k2} \phi_{,k}^{(3)},$$

$$D_i^{(3)} = \int_{-b}^b D_i x_2 (x_2^2 - b^2) dx_2 = -e_{ip} \sum_{m=1, 3, 5, \dots}^{\infty} \frac{4b^{m+4}}{(m+4)(m+2)} S_p^{(m)} + \frac{8b^5}{15} \epsilon_{2i} \phi^{(2)} - \frac{16b^7}{105} \epsilon_{ki} \phi_{,k}^{(3)},$$

$$\bar{D}_2^{(3)} = \int_{-b}^b D_2 (3x_2^2 - b^2) dx_2 = e_{2p} \sum_{m=0, 2, 4, \dots}^{\infty} \frac{4mb^{m+3}}{(m+3)(m+1)} S_p^{(m)} - \frac{8b^5}{15} \epsilon_{k2} \phi_{,k}^{(2)} - \frac{8b^5}{5} \epsilon_{22} \phi^{(3)}. \quad (18)$$

The electric displacements in terms of strain and electric field vectors for the third-order theory are

$$D_i^{(2)} = -e_{ip} \left(\frac{4b^3}{3} S_p^{(0)} + \frac{4b^5}{15} S_p^{(2)} \right) + \frac{16b^5}{15} \epsilon_{ki} E_k^{(2)} + \frac{8b^5}{15} \epsilon_{2i} E_2^{(3)} + \frac{4b^2}{3} \epsilon_{2i} \phi_1,$$

$$\bar{D}_2^{(2)} = e_{2p} \left(\frac{4b^3}{3} S_p^{(1)} + \frac{4b^5}{5} S_p^{(3)} \right) + \frac{8b^3}{3} \epsilon_{22} E_2^{(2)} - \frac{8b^5}{15} \epsilon_{k2} E_k^{(3)},$$

$$D_i^{(3)} = -e_{ip} \left(\frac{4b^5}{15} S_p^{(1)} + \frac{4b^7}{35} S_p^{(3)} \right) - \frac{8b^5}{15} \epsilon_{2i} E_2^{(2)} + \frac{16b^7}{105} \epsilon_{ki} E_k^{(3)},$$

$$\bar{D}_2^{(3)} = e_{2p} \frac{8b^5}{15} S_p^{(2)} + \frac{8b^5}{15} \epsilon_{k2} E_k^{(2)} + \frac{8b^5}{5} \epsilon_{22} E_2^{(3)}. \quad (19)$$

Again, these equations can be expressed in tensor notations as

$$\mathbf{D}^{(k)} = \mathbf{e}_k^{(m)} \mathbf{S}^{(m)} + \epsilon_k^{(2)} \mathbf{E}^{(2)} + \epsilon_k^{(3)} \mathbf{E}^{(3)} + \epsilon^{(k)} \phi_1, \quad k = 2, 3. \quad (20)$$

In addition to the constitutive relations given in Eqs. (13) and (20), we also have the two-dimensional equations of motion (Mindlin, 1972; Wang et al., 1999) and charge as

$$T_{ij,i}^{(n)} - nT_{2j}^{(n-1)} + F_j^{(n)} = \rho \sum_{m=0}^{\infty} B_{mn} [1 + (m+n+1)R] \dot{u}_j^{(m)}, \quad n = 0, 1, 2, 3,$$

$$D_{i,i}^{(k)} - \bar{D}_2^{(k)} = 0, \quad k = 2, 3, \quad (21)$$

where ρ is the density of material and R is the mass ratio (Wang et al., 1999). It is clear that although the face traction of the plate is still considered through $F_j^{(n)}$, the face charge terms which have to be

approximated in both power and trigonometric series expansions have been totally eliminated, thus providing a precise description of the electric potential and displacement on the faces. This feature is the sole purpose of these equations.

2.3. Boundary conditions

The changes in the electric potential expansion will certainly make the boundary conditions different, particularly the ones related to the potential and charge. A proper summary of such changes will be important in the consideration of the electrodes and their requirements. To obtain proper boundary conditions, for the plate configuration shown in Fig. 1, we start with

$$\int_S [(t_j - n_i T_{ij})\delta u_j + (\sigma - n_i D_i)\delta\phi] dS = 0, \tag{22}$$

where n_i , t_j , and σ are outward normal, prescribed traction, and prescribed charge, respectively. The variation of the two-dimensional displacements is

$$\delta u_j = \sum_{n=0}^{\infty} x_2^n \delta u_j^{(n)}, \tag{23}$$

and the potential is given in (6)₁ already. However, since the displacements are expanded in power series, we only need to work on the equations related to the charge equations on the boundary.

By using (6)₁ in (22) with only the charge related equations, we have

$$\int_S (\sigma - n_i D_i) [(x_2^2 - b^2)\delta\phi^{(2)} + x_2(x_2^2 - b^2)\delta\phi^{(3)}] dS = 0, \tag{24}$$

or

$$\int_C [(\sigma^{(2)} - n_i D_i^{(2)})\delta\phi^{(2)} + (\sigma^{(3)} - n_i D_i^{(3)})\delta\phi^{(3)}] ds = 0, \tag{25}$$

where

$$\sigma^{(2)} = \int_{-b}^b \sigma(x_2^2 - b^2) dx_2, \quad \sigma^{(3)} = \int_{-b}^b \sigma x_2(x_2^2 - b^2) dx_2. \tag{26}$$

It is clear that the boundary conditions on the faces ($x_2 = \pm b$) have been taken care of by the diminishing of the potential. For the cylindrical faces (edges), we have

$$\sigma^{(2)} - n_i D_i^{(2)} = 0, \quad \sigma^{(3)} - n_i D_i^{(3)} = 0, \tag{27}$$

or alternatively

$$\phi^{(2)} = \bar{\phi}^{(2)}, \quad \phi^{(3)} = \bar{\phi}^{(3)}, \tag{28}$$

where $\bar{\phi}^{(k)}$ ($k = 2, 3$) are prescribed potentials.

These equations are the complete set for the piezoelectric plate covered with electrodes. Displacement and potential variables up to the third-order have been considered in this derivation. For many applications, it is always necessary to eliminate some less dominant modes to preserve the strongly coupled thickness-shear and flexural vibrations. Since we are more concerned in the finite element

implementation of these equations, we leave further work on the simplification and reduction to the future. We also want to emphasize that the derivation of these equations is consistent with higher order Mindlin plate theory, which has been implemented in our finite element analysis of crystal resonators (Yong et al., 1996a; Wang et al., 1999) with success. We expect that the two groups of equations can be combined so the analysis of plates with partial electrodes can be carried out smoothly.

2.4. Capacitance

For a crystal resonator driven by an alternating voltage, the electrical properties can be obtained through the analysis of the forced vibrations. The mechanical displacement and electric potential solutions from such analysis can be used for the calculation of the motional capacitance, which in turn can be used for the evaluation of inductance and other quantities. In addition to measuring the overall quality of the resonator, these properties can be used in the determination of the strength of resonance and coupling of modes.

For the calculation of capacitance, we follow Lee and Lin (1998) with the charge equation

$$\int_V D_{i,i} dV = 0. \quad (29)$$

For a small box bounded by $x_1'' < x_1 < x_1'$, $-b < x_2'' < x_2 < x_2' < b$, considering $D_{1,1} = D_{3,3} = 0$ due to the uniform distribution of electric potential on the faces, the above equation can be rewritten as

$$\int_A [D_2(x_2') - D_2(x_2'')] dA = 0. \quad (30)$$

This implies that on all the planes parallel to the faces, the charge should be the same. Based on this observation, we have

$$\int_V f(x_2) D_2 dV = \int_{-b}^b f(x_2) dx_2 \int_A D_2 dA, \quad (31)$$

or

$$\int_A D_2 dA = \frac{\int_A \int_{-b}^b f(x_2) D_2 dx_2 dA}{\int_{-b}^b f(x_2) dx_2}. \quad (32)$$

The total surface charge on the face is

$$Q = \int_A D_2 dA, \quad (33)$$

where A is the electroded area.

In this study, we have noticed that

$$D_2^{(2)} = \int_{-b}^b (x_2^2 - b^2) D_2 dx_2, \quad (34)$$

or the weighting function is $f(x_2) = x_2^2 - b^2$. Through integration of (32), the charge is given as

$$Q = \frac{3}{4b^3} \int_A D_2^{(2)} dA. \tag{35}$$

With $D_2^{(2)}$ given in (19)₁, we have

$$\begin{aligned} Q &= \frac{3}{4b^3} \int_A \left[-e_{2p} \left(\frac{4b^3}{3} S_p^{(0)} + \frac{4b^5}{15} S_p^{(2)} \right) - \frac{16b^5}{15} \epsilon_{k2} \phi_{,k}^{(2)} - \frac{8b^5}{15} \epsilon_{22} \phi^{(3)} + \frac{4b^2}{3} \epsilon_{22} \phi_1 \right] dA \\ &= \frac{\epsilon_{22} A}{b} \phi_1 - \int_A \left[e_{2p} \left(S_p^{(0)} + \frac{b^2}{5} S_p^{(2)} \right) + \frac{4b^2}{5} \epsilon_{k2} \phi_{,k}^{(2)} + \frac{2b^2}{5} \epsilon_{22} \phi^{(3)} \right] dA. \end{aligned} \tag{36}$$

The static and motional capacitances and capacitance ratio for the electroded plate are

$$C_s = \frac{\epsilon_{22} A}{2b}, \quad C_m = \frac{Q}{2\phi_1}, \quad C_r = \frac{C_m}{C_s}, \tag{37}$$

where A is the area of the electroded plate.

The capacitance ratio from these equations is given as

$$C_r = 1 - \frac{b}{\phi_1 \epsilon_{22} A} \int_A \left[e_{2p} \left(S_p^{(0)} + \frac{b^2}{5} S_p^{(2)} \right) + \frac{4b^2}{5} \epsilon_{k2} \phi_{,k}^{(2)} + \frac{2b^2}{5} \epsilon_{22} \phi^{(3)} \right] dA. \tag{38}$$

3. Finite element formulation

For the two-dimensional solutions of the vibration equations of an electroded plate that we present in the previous section, we turn to the finite element method, as we did in the free mechanical and piezoelectric vibrations of crystal plates (Wang et al., 1999). However, the electrodes were only considered for its mass effect with the neglect of the equal potential face conditions. The implementation of the equation we derived here will provide a more suitable approach, although the piezoelectric effect, with or without the consideration of the electrodes, is probably too small to have a noticeable impact on the frequency solutions, as we have concluded before (Wang et al., 1999).

The variational equations of motion and charge, which can be derived from Eq. (21) by following a standard procedure (Wang et al., 1999), upon proper manipulation, can be written as

$$\begin{aligned} \int_A \left\{ T_{ij}^{(n)} \delta S_{ij}^{(n)} + \sum_{m=0}^{\infty} B_{mm} [1 + (m + n + 1)R] \rho \ddot{u}_j^{(m)} \delta u_j^{(n)} \right\} dA &= \int_C n_i T_{ij}^{(n)} \delta u_j^{(n)} ds + \int_A F_j^{(n)} \delta u_j^{(n)} dA, \\ \int_A \left(D_k^{(2)} \delta E_k^{(2)} + \bar{D}_2^{(2)} \delta E_2^{(2)} + D_k^{(3)} \delta E_k^{(3)} + \bar{D}_2^{(3)} \delta E_2^{(3)} \right) dA &= - \int_C n_i \left(D_i^{(2)} \delta \phi^{(2)} + D_i^{(3)} \delta \phi^{(3)} \right) ds, \end{aligned} \tag{39}$$

where R is the mass ratio and n_i ($i = 1, 3$) is the outward normal of the cylindrical surface.

For piezoelectric materials, the virtual electric enthalpy density is defined as (Mindlin, 1972)

$$\delta H = T_{ij} \delta S_{ij} - D_i \delta E_i. \tag{40}$$

With the two-dimensional variables, the variational equations in (39) can be translated into

$$\begin{aligned}
& \int_A \left\{ T_{ij}^{(n)} \delta S_{ij}^{(n)} - \left(D_k^{(2)} \delta E_k^{(2)} + \bar{D}_2^{(2)} \delta E_2^{(2)} + D_k^{(3)} \delta E_k^{(3)} + \bar{D}_2^{(3)} \delta E_2^{(3)} \right) \right. \\
& \quad \left. + \sum_{m=0}^{\infty} B_{mm} [1 + (m+n+1)R] \rho \ddot{u}_j^{(m)} \delta u_j^{(n)} \right\} dA \\
& = \int_A F_j^{(n)} \delta u_j^{(n)} dA + \int_C n_i \left[T_{ij}^{(n)} \delta u_j^{(n)} + \left(D_i^{(2)} \delta \phi^{(2)} + D_i^{(3)} \delta \phi^{(3)} \right) \right] ds.
\end{aligned} \tag{41}$$

It can be seen that the mechanical and electric variables are being neatly incorporated into one equation. With some proper definitions and arrangements, we should be able to combine them into one set of independent variables as generalized displacements and field quantities, thus resulting in a generalized approach which is different with the traditional technique where the two equations are solved separately through iteration (Wang et al., 1999). This is the base of our generalized finite element formulation and implementation of the electroded piezoelectric plate theory.

As the starting point, we define the generalized displacement vector, which includes both mechanical displacements and electric potentials, for the third-order theory as

$$\mathbf{u} = \left\{ u_1^{(0)}, u_2^{(0)}, u_3^{(0)}, u_1^{(1)}, u_2^{(1)}, u_3^{(1)}, u_1^{(2)}, u_2^{(2)}, u_3^{(2)}, \phi^{(2)}, u_1^{(3)}, u_2^{(3)}, u_3^{(3)}, \phi^{(3)} \right\}_{14 \times 1}, \tag{42}$$

and the corresponding generalized strain vector as

$$\mathbf{S} = \left\{ \mathbf{S}^{(0)}, \mathbf{S}^{(1)}, \mathbf{S}^{(2)}, \mathbf{E}^{(2)}, \mathbf{S}^{(3)}, \mathbf{E}^{(3)} \right\}_{30 \times 1}, \tag{43}$$

with

$$\begin{aligned}
\mathbf{S}^{(k)} & = \left\{ S_1^{(k)}, S_2^{(k)}, S_3^{(k)}, S_4^{(k)}, S_5^{(k)}, S_6^{(k)} \right\}_{6 \times 1}, \quad k = 0, 1, 2, 3, \\
\mathbf{E}^{(m)} & = \left\{ E_2^{(m)}, E_1^{(m)}, E_3^{(m)} \right\}_{3 \times 1}, \quad m = 2, 3.
\end{aligned} \tag{44}$$

In comparison to the generalized formulation of the free piezoelectric vibrations (Wang et al., 1999), we see that the zeroth- and first-order electric potentials $\phi^{(0)}$ and $\phi^{(1)}$ are no longer present. This reminds us that special care has to be taken if the plate is partially electroded, which is a problem of practical importance.

As a result, the generalized strain and displacement vectors are related to each other by

$$\mathbf{S} = \partial_S \mathbf{u}, \tag{45}$$

where the matrix operator is defined as

$$\partial_S = \begin{bmatrix} \partial_u & \partial_u^{(1)} & 0 & 0 & 0 & 0 \\ 0 & \partial_u & \partial_u^{(2)} & 0 & 0 & 0 \\ 0 & 0 & \partial_u & 0 & \partial_u^{(3)} & 0 \\ 0 & 0 & 0 & \partial_\phi & 0 & 0 \\ 0 & 0 & 0 & 0 & \partial_u & 0 \\ 0 & 0 & 0 & 0 & 0 & \partial_\phi \end{bmatrix}_{30 \times 14}, \tag{46}$$

with submatrices defined as

$$\partial_u = \begin{bmatrix} \frac{\partial}{\partial x_1} & 0 & 0 \\ 0 & 0 & 0 \\ 0 & 0 & \frac{\partial}{\partial x_3} \\ 0 & \frac{\partial}{\partial x_3} & 0 \\ \frac{\partial}{\partial x_3} & 0 & \frac{\partial}{\partial x_1} \\ 0 & \frac{\partial}{\partial x_1} & 0 \end{bmatrix}_{6 \times 3}, \quad \partial_u^{(n+1)} = (n+1) \begin{bmatrix} 0 & 0 & 0 \\ 0 & 1 & 0 \\ 0 & 0 & 0 \\ 0 & 0 & 1 \\ 0 & 0 & 0 \\ 1 & 0 & 0 \end{bmatrix}_{6 \times 3}, \quad \partial_\phi = - \begin{bmatrix} 1 \\ \frac{\partial}{\partial x_1} \\ \frac{\partial}{\partial x_3} \end{bmatrix}_{3 \times 1}. \quad (47)$$

Similarly, we define the generalized stress vector

$$\mathbf{T} = \{\mathbf{T}^{(0)}, \mathbf{T}^{(1)}, \mathbf{T}^{(2)}, \mathbf{D}^{(2)}, \mathbf{T}^{(3)}, \mathbf{D}^{(3)}\}_{30 \times 1}, \quad (48)$$

where

$$\mathbf{T}^{(k)} = \{T_1^{(k)}, T_2^{(k)}, T_3^{(k)}, T_4^{(k)}, T_5^{(k)}, T_6^{(k)}\}_{6 \times 1}, \quad k = 0, 1, 2, 3,$$

$$\mathbf{D}^{(m)} = \{\bar{D}_2^{(m)}, D_1^{(m)}, D_3^{(m)}\}_{3 \times 1}, \quad m = 2, 3. \quad (49)$$

Now the constitutive relations can be expressed in matrix form as

$$\mathbf{T} = \mathbf{CS} + \mathbf{e}_1 \phi_1, \quad (50)$$

where

$$\mathbf{C} = \begin{bmatrix} B_{00}\mathbf{c} & 0 & B_{02}\mathbf{c} & -\mathbf{e}_0^{(2)} & 0 & 0 \\ 0 & B_{11}\mathbf{c} & 0 & -\mathbf{e}_1^{(2)} & B_{13}\mathbf{c} & -\mathbf{e}_1^{(3)} \\ B_{20}\mathbf{c} & 0 & B_{22}\mathbf{c} & -\mathbf{e}_2^{(2)} & 0 & -\mathbf{e}_2^{(3)} \\ \mathbf{e}_2^{(0)} & \mathbf{e}_2^{(1)} & \mathbf{e}_2^{(2)} & \epsilon_2^{(2)} & \bar{\mathbf{e}}_2^{(3)} & \epsilon_2^{(3)} \\ 0 & B_{31}\mathbf{c} & 0 & -\bar{\mathbf{e}}_3^{(2)} & B_{33}\mathbf{c} & -\mathbf{e}_3^{(3)} \\ 0 & \mathbf{e}_3^{(1)} & \mathbf{e}_3^{(2)} & \epsilon_3^{(2)} & \mathbf{e}_3^{(3)} & \epsilon_3^{(3)} \end{bmatrix}_{30 \times 30}, \quad \mathbf{e}_1 = \begin{bmatrix} -\mathbf{e}^{(0)} \\ 0 \\ -\mathbf{e}^{(2)} \\ \epsilon^{(2)} \\ 0 \\ 0 \end{bmatrix}_{30 \times 1}. \quad (51)$$

It should be noticed that $\bar{\mathbf{e}}_3^{(2)}$ and $\mathbf{e}_3^{(2)}$ are different quantities.

The material constant submatrices, as appears here and in the previous section, are

$$\mathbf{e}_0^{(2)} = -\frac{4b^3}{3}[\mathbf{0}, \mathbf{e}_1, \mathbf{e}_3], \quad \mathbf{e}_1^{(2)} = \frac{4b^3}{3}[\mathbf{e}_2, \mathbf{0}, \mathbf{0}],$$

$$\mathbf{e}_1^{(3)} = \mathbf{e}_2^{(2)} = -\frac{4b^5}{15}[\mathbf{0}, \mathbf{e}_1, \mathbf{e}_3], \quad \bar{\mathbf{e}}_3^{(2)} = \frac{4b^5}{5}[\mathbf{e}_2, \mathbf{0}, \mathbf{0}],$$

$$\mathbf{e}_2^{(3)} = \frac{8b^5}{15}[\mathbf{e}_2, \mathbf{0}, \mathbf{0}], \quad \mathbf{e}_3^{(3)} = -\frac{4b^7}{35}[\mathbf{0}, \mathbf{e}_1, \mathbf{e}_3]$$

$$\epsilon_2^{(2)} = \frac{16b^5}{15} \begin{bmatrix} \frac{5}{2b^2}\epsilon_{22} & 0 & 0 \\ 0 & \epsilon_{11} & \epsilon_{31} \\ 0 & \epsilon_{13} & \epsilon_{33} \end{bmatrix},$$

$$\epsilon_2^{(3)} = \frac{8b^5}{15} \begin{bmatrix} 0 & -\epsilon_{12} & -\epsilon_{32} \\ \epsilon_{21} & 0 & 0 \\ \epsilon_{23} & 0 & 0 \end{bmatrix},$$

$$\epsilon_3^{(3)} = \frac{16b^7}{105} \begin{bmatrix} \frac{35}{2b^2}\epsilon_{22} & 0 & 0 \\ 0 & \epsilon_{11} & \epsilon_{31} \\ 0 & \epsilon_{13} & \epsilon_{33} \end{bmatrix}, \quad \epsilon^{(2)} = \frac{4b^2}{3}\epsilon_2,$$

$$\mathbf{e}^{(0)} = -2\mathbf{e}_2, \quad \mathbf{e}^{(2)} = -\frac{2b^2}{3}\mathbf{e}_2,$$

$$\mathbf{e}_i = \{e_{i1}, e_{i2}, e_{i3}, e_{i4}, e_{i5}, e_{i6}\}, \quad i = 1, 2, 3,$$

$$\epsilon_1 = \{\epsilon_{22}, 0, 0\}, \quad \epsilon_2 = \{0, \epsilon_{21}, \epsilon_{23}\}, \quad (52)$$

The variational equation (41) in matrix notations is

$$\int_A \delta \mathbf{S}^T \bar{\mathbf{D}} \mathbf{S} dA + \int_A \delta \bar{\mathbf{u}}^T \mathbf{m} \ddot{\mathbf{u}} dA = \int_A \delta \mathbf{S}^T \bar{\mathbf{e}}_1 \phi_1 dA + \int_A \delta \bar{\mathbf{u}}^T \mathbf{F} dA + \int_C \delta \bar{\mathbf{u}}^T \mathbf{f} ds, \quad (53)$$

where

$$\bar{\mathbf{D}} = \begin{bmatrix} B_{00}\mathbf{c} & 0 & B_{02}\mathbf{c} & -\mathbf{e}_0^{(2)} & 0 & 0 \\ 0 & B_{11}\mathbf{c} & 0 & -\mathbf{e}_1^{(2)} & B_{13}\mathbf{c} & -\mathbf{e}_1^{(3)} \\ B_{20}\mathbf{c} & 0 & B_{22}\mathbf{c} & -\mathbf{e}_2^{(2)} & 0 & -\mathbf{e}_2^{(3)} \\ -\mathbf{e}_2^{(0)} & -\mathbf{e}_2^{(1)} & -\mathbf{e}_2^{(2)} & -\epsilon_2^{(2)} & -\bar{\mathbf{e}}_2^{(3)} & -\epsilon_2^{(3)} \\ 0 & B_{31}\mathbf{c} & 0 & -\bar{\mathbf{e}}_3^{(2)} & B_{33}\mathbf{c} & -\mathbf{e}_3^{(3)} \\ 0 & -\mathbf{e}_3^{(1)} & -\mathbf{e}_3^{(2)} & -\epsilon_3^{(2)} & -\mathbf{e}_3^{(3)} & -\epsilon_3^{(3)} \end{bmatrix}_{30 \times 30}, \quad \bar{\mathbf{e}}_1 = \begin{bmatrix} \mathbf{e}^{(0)} \\ \mathbf{0} \\ \mathbf{e}^{(2)} \\ \epsilon^{(2)} \\ \mathbf{0} \\ \mathbf{0} \end{bmatrix}_{30 \times 1}, \quad (54)$$

$$\mathbf{m} = \begin{bmatrix} \mathbf{m}_0^{(0)} & 0 & \mathbf{m}_0^{(2)} & 0 & 0 & 0 \\ 0 & \mathbf{m}_1^{(1)} & 0 & 0 & \mathbf{m}_1^{(3)} & 0 \\ \mathbf{m}_2^{(0)} & 0 & \mathbf{m}_2^{(2)} & 0 & 0 & 0 \\ 0 & 0 & 0 & 0 & 0 & 0 \\ 0 & \mathbf{m}_3^{(1)} & 0 & 0 & \mathbf{m}_3^{(3)} & 0 \\ 0 & 0 & 0 & 0 & 0 & 0 \end{bmatrix}_{14 \times 14},$$

$$\mathbf{m}_m^{(n)} = \rho B_{mn} [1 + (m + n + 1)R] \mathbf{I}_{3 \times 3}.$$

The definitions for the boundary terms \mathbf{F} and \mathbf{f} in Eq. (53) can be found in Eq. (41). For the forced vibration analysis, particular attention should be directed to the excitation force term appearing to the right-hand side of Eq. (53).

Now we discretize the variational equation (53) with

$$\mathbf{u} = \mathbf{N}\mathbf{U}, \quad \mathbf{B} = \partial_S \mathbf{N}, \tag{55}$$

where \mathbf{N} and \mathbf{U} are interpolation function and discretized displacement matrices, respectively. The discretized variational equation is

$$\int_A \mathbf{B}^T \bar{\mathbf{D}} \mathbf{B} \, dA \, \mathbf{U} + \int_A \mathbf{N}^T \mathbf{m} \mathbf{N} \, dA \, \ddot{\mathbf{U}} = \int_A \mathbf{B}^T \bar{\mathbf{e}}_1 \, dA \, \phi_1 + \int_A \mathbf{N}^T \mathbf{F} \, dA + \int_C \mathbf{N}^T \mathbf{f} \, ds, \tag{56}$$

or

$$\mathbf{K}\mathbf{U} + \mathbf{M}\ddot{\mathbf{U}} = \mathbf{F}_E + \mathbf{F}_A + \mathbf{F}_C, \tag{57}$$

where

$$\begin{aligned} \mathbf{K} &= \int_A \mathbf{B}^T \bar{\mathbf{D}} \mathbf{B} \, dA, & \mathbf{M} &= \int_A \mathbf{N}^T \mathbf{m} \mathbf{N} \, dA, \\ \mathbf{F}_E &= \int_A \mathbf{B}^T \bar{\mathbf{e}}_1 \, dA \, \phi_1, & \mathbf{F}_A &= \int_A \mathbf{N}^T \mathbf{F} \, dA, & \mathbf{F}_C &= \int_C \mathbf{N}^T \mathbf{f} \, ds, \end{aligned} \tag{58}$$

are the stiffness matrix, mass matrix, excitation force vector, face force vector, and edge force vector, respectively. Details of these matrices can be found in our previous paper (Wang et al., 1999).

If the steady vibration is assumed, we have

$$\mathbf{K}\mathbf{U} - \omega^2 \mathbf{M}\mathbf{U} = \mathbf{F}_E + \mathbf{F}_A + \mathbf{F}_C, \tag{59}$$

where the vibration frequency ω is usually normalized by the fundamental thickness frequency

$$\omega_0 = \frac{\pi}{2b} \sqrt{\frac{c_{66}}{\rho}}. \tag{60}$$

The free vibrations, or the eigenvalue problem, can be deduced from (59) by setting all the force vectors to zero.

For the computation of the stiffness matrix, we have

$$\mathbf{B} = \begin{bmatrix}
 N_{i,1} & 0 & 0 & 0 & 0 & 0 & 0 & 0 & 0 & 0 & 0 & 0 & 0 & 0 \\
 0 & 0 & 0 & 0 & N_i & 0 & 0 & 0 & 0 & 0 & 0 & 0 & 0 & 0 \\
 0 & 0 & N_{i,3} & 0 & 0 & 0 & 0 & 0 & 0 & 0 & 0 & 0 & 0 & 0 \\
 0 & N_{i,3} & 0 & 0 & 0 & N_i & 0 & 0 & 0 & 0 & 0 & 0 & 0 & 0 \\
 N_{i,3} & 0 & N_{i,1} & 0 & 0 & 0 & 0 & 0 & 0 & 0 & 0 & 0 & 0 & 0 \\
 0 & N_{i,1} & 0 & N_i & 0 & 0 & 0 & 0 & 0 & 0 & 0 & 0 & 0 & 0 \\
 0 & 0 & 0 & N_{i,1} & 0 & 0 & 0 & 0 & 0 & 0 & 0 & 0 & 0 & 0 \\
 0 & 0 & 0 & 0 & 0 & 0 & 0 & 2N_i & 0 & 0 & 0 & 0 & 0 & 0 \\
 0 & 0 & 0 & 0 & 0 & N_{i,3} & 0 & 0 & 0 & 0 & 0 & 0 & 0 & 0 \\
 0 & 0 & 0 & 0 & N_{i,3} & 0 & 0 & 0 & 2N_i & 0 & 0 & 0 & 0 & 0 \\
 0 & 0 & 0 & N_{i,3} & 0 & N_{i,1} & 0 & 0 & 0 & 0 & 0 & 0 & 0 & 0 \\
 0 & 0 & 0 & 0 & N_{i,1} & 0 & 2N_i & 0 & 0 & 0 & 0 & 0 & 0 & 0 \\
 0 & 0 & 0 & 0 & 0 & 0 & N_{i,1} & 0 & 0 & 0 & 0 & 0 & 0 & 0 \\
 0 & 0 & 0 & 0 & 0 & 0 & 0 & 0 & 0 & 0 & 0 & 3N_i & 0 & 0 \\
 0 & 0 & 0 & 0 & 0 & 0 & 0 & 0 & N_{i,3} & 0 & 0 & 0 & 0 & 0 \\
 0 & 0 & 0 & 0 & 0 & 0 & 0 & 0 & N_{i,3} & 0 & 0 & 0 & 3N_i & 0 \\
 0 & 0 & 0 & 0 & 0 & 0 & 0 & 0 & N_{i,3} & 0 & N_{i,1} & 0 & 0 & 0 \\
 0 & 0 & 0 & 0 & 0 & 0 & 0 & 0 & N_{i,1} & 0 & 0 & 3N_i & 0 & 0 \\
 0 & 0 & 0 & 0 & 0 & 0 & 0 & 0 & 0 & 0 & -N_i & 0 & 0 & 0 \\
 0 & 0 & 0 & 0 & 0 & 0 & 0 & 0 & 0 & 0 & -N_{i,1} & 0 & 0 & 0 \\
 0 & 0 & 0 & 0 & 0 & 0 & 0 & 0 & 0 & 0 & -N_{i,3} & 0 & 0 & 0 \\
 0 & 0 & 0 & 0 & 0 & 0 & 0 & 0 & 0 & 0 & 0 & N_{i,1} & 0 & 0 \\
 0 & 0 & 0 & 0 & 0 & 0 & 0 & 0 & 0 & 0 & 0 & 0 & 0 & 0 \\
 0 & 0 & 0 & 0 & 0 & 0 & 0 & 0 & 0 & 0 & 0 & 0 & N_{i,3} & 0 \\
 0 & 0 & 0 & 0 & 0 & 0 & 0 & 0 & 0 & 0 & 0 & N_{i,3} & 0 & 0 \\
 0 & 0 & 0 & 0 & 0 & 0 & 0 & 0 & 0 & 0 & 0 & N_{i,3} & 0 & N_{i,1} \\
 0 & 0 & 0 & 0 & 0 & 0 & 0 & 0 & 0 & 0 & 0 & 0 & N_{i,1} & 0 \\
 0 & 0 & 0 & 0 & 0 & 0 & 0 & 0 & 0 & 0 & 0 & 0 & 0 & -N_i \\
 0 & 0 & 0 & 0 & 0 & 0 & 0 & 0 & 0 & 0 & 0 & 0 & 0 & -N_{i,1} \\
 0 & 0 & 0 & 0 & 0 & 0 & 0 & 0 & 0 & 0 & 0 & 0 & 0 & -N_{i,3}
 \end{bmatrix} \quad 30 \times 14 \quad (61)$$

Finally, with the displacement solutions from Eq. (59), we can also formulate the capacitance ratio into matrix format as

$$C_r = 1 - \frac{b}{\phi_1 \epsilon_{22} A} \int_A \mathbf{e}_2 \mathbf{B} \mathbf{U} \, dA, \quad (62)$$

where

$$\mathbf{e}_2 = \left[\mathbf{e}_2^T, \mathbf{0}, \frac{b^2}{5} \mathbf{e}_2^T, -\frac{4b^2}{5} \epsilon_2^T, \mathbf{0}, -\frac{2b^2}{5} \epsilon_1^T \right]_{1 \times 30}. \quad (63)$$

4. Numerical examples

With the successful derivation of the new equations and the systematic implementation in the finite element analysis, it is necessary, as it has always been, to verify the computational results with existing

experimental data. The validated equations then can be combined with other techniques for the modeling of real crystal resonators, which usually have partial electrodes and support structures in addition to the crystal plates. The computing issues concerning this implementation, such as the eigenvalue extraction, convergence, high vibration frequency, and finer mesh requirement, are the same as the piezoelectric plates we have considered before (Wang et al., 1999). What is unique here is that the forced vibrations also require a linear solver for the large and sparse linear equation, which is associated with the eigenvalue problem. Generally speaking, the number of elements and resulting equations with the third-order plate theory are very large and proportional to the aspect ratios because of the high vibration frequency. However, the focus of this study is to demonstrate the effectiveness of the new theory in the prediction of the resonance frequencies and the capacitance ratio. Computational results, fortunately, can be compared to the existing experimental data to validate the theory through following examples.

4.1. Frequency spectrum

The first example we present here is the comparison of the frequency spectrum of a crystal plate which was studied experimentally by Koga (1963) before. In our computation, the four-node element, which also has two incompatible nodes, is used with the truncation of the third-order theory (Wang et al., 1999), although the program we have can handle other elements, such as the nine- and sixteen-node types. In the frequency spectrum, or the frequency versus the length to thickness ratio a/b , shown in Fig. 2, it is found that, with a slight shift, the frequency spectra agree well. It is also easy to see that the spectrum based on the current theory is actually very close to the previous ones with pure mechanical or piezoelectric vibrations (Wang et al., 1999). The piezoelectric effect, as we found earlier, is indeed very small. However, the comparison concludes that the current theory will generally predict the resonance

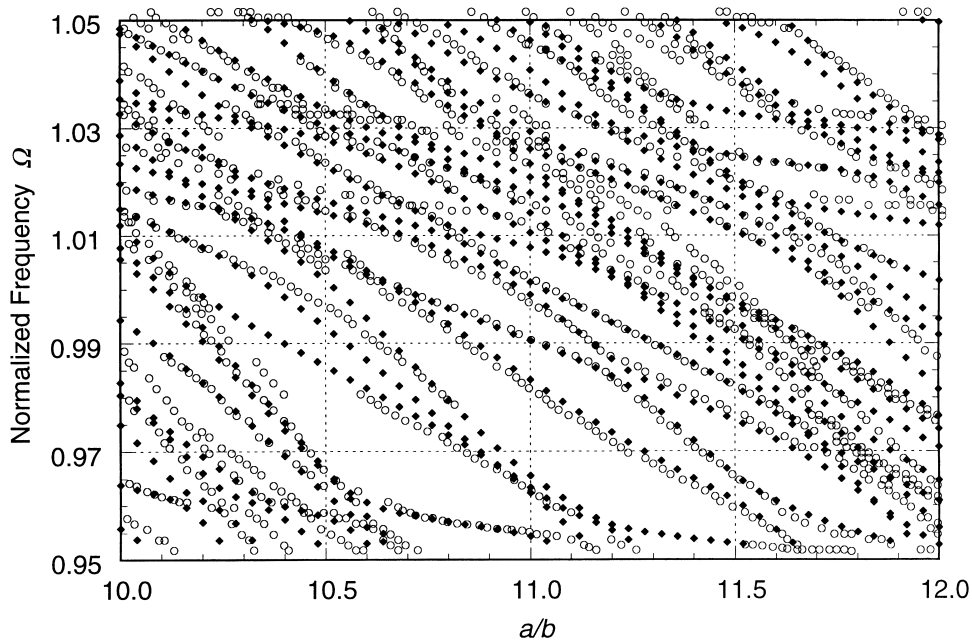


Fig. 2. Normalized frequency Ω vs. length to thickness ratio a/b of crystal plates with $c/b = 16.3660$ and $R = 0.008$ in comparison with experimental data (○) from Koga (1963).

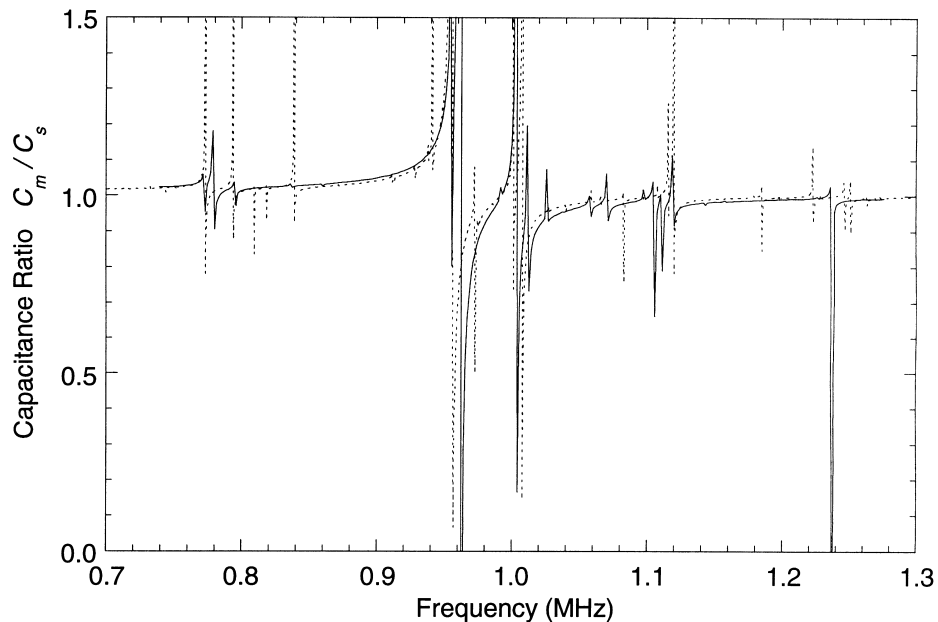


Fig. 3. Capacitance ratio of an electroded crystal plate with $a/b = 8.0391$, $c/b = 4.0229$, and $R = 0.003$. The dotted lines are measurements by Sekimoto et al. (1992).

frequencies with considerable accuracy. This is also a reminder for us to study more complicated configurations with pure mechanical vibrations due to its dominance.

4.2. Capacitance ratios

The ultimate goal of the new theory, as we stated in the beginning, is to study the forced vibrations of crystal resonators. The finite element formulation and implementation of the equations for this purpose have made it possible for us to obtain the displacement and potential solutions excited by the driving voltage on the electrodes. In turn, the solutions can be used for the calculations we formulated earlier. To demonstrate the effectiveness of the current theory, we computed the capacitance ratios of three crystal plate samples of different aspect ratios and compared them with the experimental data obtained by Sekimoto et al. (1992) in Figs. 3–5. Again, small shifts have been made to match the major vibration modes, fundamental thickness-shear in particular, more accurately. From the three samples, we find that generally the computational results agree well with the measured ones. The noticeable discrepancies, particular in the regions away from the fundamental thickness-shear frequency (close to 1.0), could be the results of the inaccurate electrode information and fundamental deficiency in higher frequency. Currently we are working on means to make the resonance frequency more accurate in a broad range and for various electrodes. The effect of the electrodes could be significant if the mass ratio is higher, because the coupling of the modes and consequently the frequency spectrum will be changed.

5. Conclusions

In summary, we believe that the current theory is suitable for the study of the electroded piezoelectric plates as it is based on a rigorous derivation of the equations from basic principles. Although we

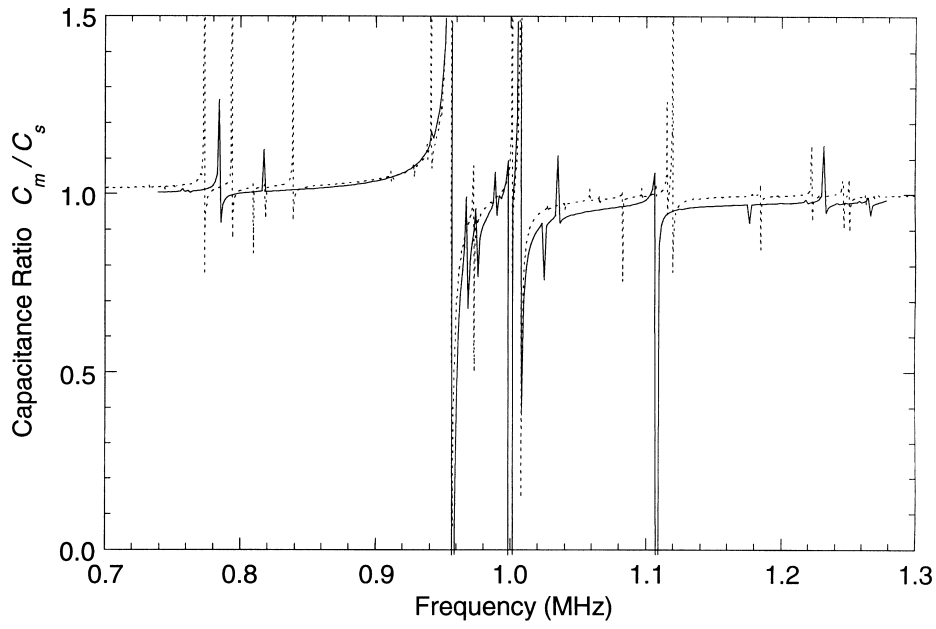


Fig. 4. Capacitance ratio of an electroded crystal plate with $a/b = 8.0391$, $c/b = 5.7571$, and $R = 0.003$. The dotted lines are measurements by Sekimoto et al. (1992).

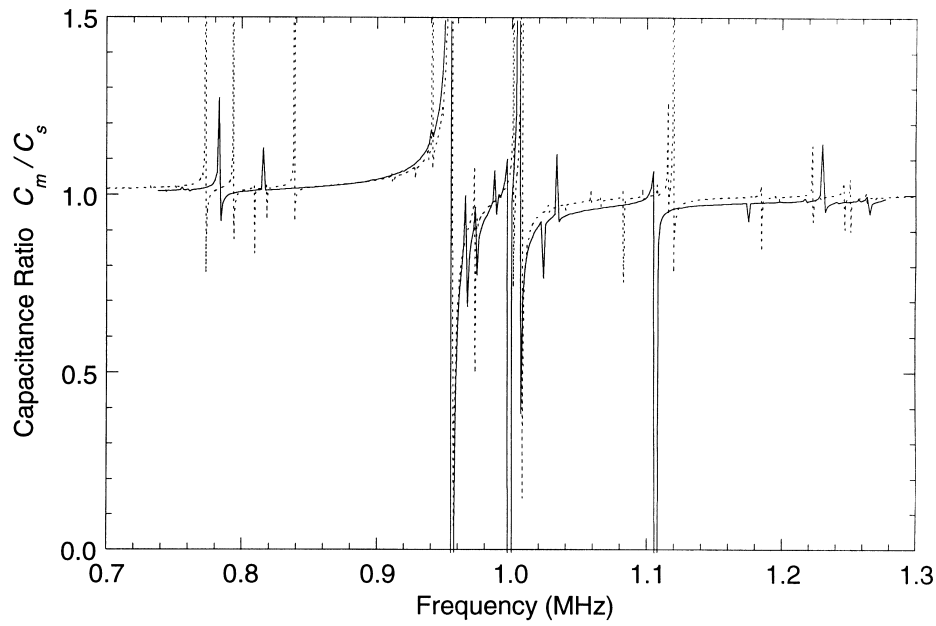


Fig. 5. Capacitance ratio of an electroded crystal plate with $a/b = 8.0391$, $c/b = 8.0599$, and $R = 0.003$. The dotted lines are measurements by Sekimoto et al. (1992).

concentrate on the third-order theory for the finite element application, it can be tailored and truncated, as most analytical solution techniques require, for the one-dimensional approximate solutions. This theory is particularly advantageous if the partially electroded plates are to be studied because the identical definitions of the higher order potentials and displacements can be chosen to satisfy the complicated boundary conditions in different regions in a natural manner. Thus it is clear that the theory is compatible to the Mindlin plate theory in cases where there are no electrodes. The same application can be found in the finite element implementation, which is the only method for precise two-dimensional solutions for plates with complicated geometry. These solutions, as we have shown here, can be used for the calculation of the electrical properties of resonators. The theory can also be applied to similar problems if the electrodes of the plate need to be considered precisely.

The sole purpose of the new theory is to simplify the electrical boundary conditions if there are electrodes on the piezoelectric plate. Because only the electrical potential expansion is modified, the effect on the mechanical equations should be very small. In other words, the Mindlin plate theory is well preserved while the electrical boundary conditions are easily handled. As demonstrated in the finite element implementation, these equations can be conveniently combined with the Mindlin plate theory for the analysis of partially electroded piezoelectric plates.

Finally, we want to point out that though it is important, at this stage the mechanical effects of the electrodes are not considered if the small discrepancies on the capacitance ratios are noted. A more satisfactory approach will include both the mass and stiffness effects of thicker electrodes.

Acknowledgements

The first author thanks Prof. Jiashi Yang of University of Nebraska, Lincoln, for many helpful discussions. The authors are grateful for the experimental data provided by Prof. Watanabe and Sekimoto of Tokyo Metropolitan University.

References

- Koga, I., 1963. Radio-frequency vibrations of rectangular *AT*-cut quartz plates. *J. Appl. Phys* 34, 2357–2365.
- Lee, P.C.Y., Lin, W.S., 1998. Piezoelectrically forced vibrations of electroded, doubly rotated crystal plates. *J. Appl. Phys* 83, 7822–7833.
- Lee, P.C.Y., Syngellakis, S., Hou, J.P., 1987. A two-dimensional theory for high-frequency vibrations of piezoelectric crystal plates with or without electrodes. *J. Appl. Phys* 61, 1249–1262.
- Lee, P.C.Y., Wang, J., 1996. Piezoelectrically forced thickness-shear and flexural vibrations of contoured quartz resonators. *J. Appl. Phys* 79, 3411–3422.
- Lee, P.C.Y., Yu, J.-D., 1998. Governing equations for a piezoelectric plate with graded properties across the thickness. *IEEE Trans. Ultrason., Ferroelec., Freq. Contr* 45, 236–250.
- Mindlin, R.D., 1955. *An Introduction to the Mathematical Theory of Vibrations of Elastic Plates*. U.S. Army Signal Corps Engineering Laboratories, Fort Monmouth, NJ.
- Mindlin, R.D., 1972. High frequency vibrations of piezoelectric crystal plates. *Int. J. Solids Struct* 8, 895–906.
- Mindlin, R.D., 1984. Frequencies of piezoelectrically forced vibrations of electroded, doubly rotated, quartz plates. *Int. J. Solids Struct* 20, 141–157.
- Sekimoto, H., Watanabe, Y., Nakazawa, M., 1992. Forced vibrations of thickness-flexure, face-shear and face-flexure in rectangular *AT*-cut quartz plates. In: *Proceedings of 1992 IEEE Frequency Control Symposium*, 532–536.
- Tiersten, H.F., 1969. *Linear Piezoelectric Plate Vibrations*. Plenum Press, New York.
- Tiersten, H.F., 1993. Equations for the extension and flexure of relatively thin electrostatic plates undergoing larger electric fields. In: Lee, J.S., Maugin, G.A., Shindo, Y. (Eds.), *Mechanics of Electromagnetic Materials and Structures*. ASME, New York, pp. 21–34 AMD Vol. 161, MD Vol. 42.
- Tiersten, H.F., Mindlin, R.D., 1962. Forced vibrations of piezoelectric crystal plates. *Quart. Appl. Math* 20, 107–119.

- Wang, J., Momosaki, E., 1997. The piezoelectrically forced vibrations of *AT*-cut quartz strip resonators. *J. Appl. Phys* 81, 1868–1876.
- Wang, J., Yong, Y.-K., Imai, T., 1999. Finite element analysis of the piezoelectric vibrations of quartz plate resonators with higher order plate theory. *Int. J. Solids Struct* 36 (15), 2303–2319.
- Yang, J.S., 1999. Equations for the extension and flexure of electroelastic plates under strong electric fields. *Int. J. Solids Struct* 36, 3171–3192.
- Yong, Y.-K., Wang, J., Imai, T., Kanna, S., Momosaki, E., 1996a. A set of hierarchical finite elements for quartz plate resonators. In: *Proceedings of the 1996 IEEE Ultrasonics Symposium*, 981–985.
- Yong, Y.-K., Zhang, Z., Hou, J.P., 1996b. On the accuracy of plate theories for the prediction of unwanted modes near the fundamental thickness-shear mode. *IEEE Trans. Ultrason., Ferroelec., Freq. Contr* 43, 888–892.